analytical chemistry

Article

Cite This: *Anal. Chem.* 2019, 91, 13096−13104

pubs.acs.org/ac

Cavity-Enhanced Raman and Helmholtz Resonator Photoacoustic Spectroscopy to Monitor the Mixed Sugar Metabolism of *E. coli*

George D. Metcalfe,[†] Saeed Alahmari,[†] Thomas W. Smith,[†,‡] and Michael Hippler*[,†]

[†]Department of Chemistry, University of Sheffield, Sheffield S3 7HF, U.K.

[‡]Water and Environmental Engineering Group, Faculty of Engineering and Physical Sciences, University of Southampton, Southampton SO17 1BJ, U.K.

ABSTRACT: We introduce and compare two powerful new techniques for headspace gas analysis above bacterial batch cultures by spectroscopy, Raman spectroscopy enhanced in an optical cavity (CERS), and photoacoustic detection in a differential Helmholtz resonator (DHR). Both techniques are able to monitor O_2 and CO_2 and its isotopomers with excellent sensitivity and time resolution to characterize bacterial growth and metabolism. We discuss and show some of the shortcomings of more conventional optical density (OD) measurements if used on their own without more sophisticated complementary measurements. The spectroscopic measurements can clearly and unambiguously distinguish the main phases of bacterial growth in the two media studied, LB and M9. We demonstrate how ^{13}C isotopic labeling of sugars combined with spectroscopic detection allows the study of bacterial mixed sugar metabolism to establish whether sugars are sequentially or simultaneously metabolized. For *E. coli*, we have characterized the shift from glucose to lactose metabolism without a classic diauxic lag phase. DHR and CERS are shown to be cost-effective and highly selective analytical tools in the biosciences and in biotechnology, complementing and superseding existing conventional techniques. They also provide new capabilities for mechanistic investigations and show a great deal of promise for use in stable isotope bioassays.

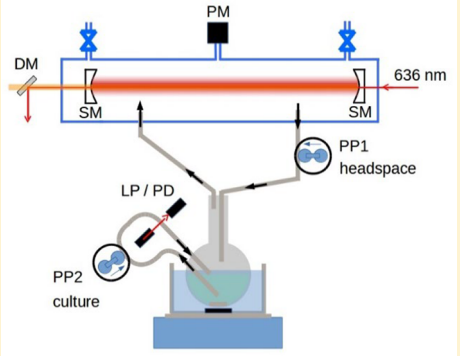

Microbial metabolism is a complex system of processes which requires interdisciplinary efforts to elucidate the function of each component and its broader connections to the whole system. Microbes consume and produce various chemical compounds. An analysis of these metabolites is an important task in microbiology; for example, it allows the study of metabolic pathways, microbial activity, enzyme reaction mechanisms, and interactions with other organisms and is essential to the optimization of industrial processes in biotechnology. In this context, the study of the mixed sugar metabolism of microbes and the resulting diauxie, where two exponential growth phases are observed, is a very relevant topic. The classic example of diauxic growth was first described by Monod after presenting *Escherichia coli* (*E. coli*) with a mixture of glucose and lactose.[1,2] Monod observed the biphasic exponential growth of *E. coli*, intermittent with a lag phase of minimal growth, due to the sequential consumption of glucose followed by lactose. Glucose is the preferred carbon source for *E. coli* as well as many other organisms.[3] These microbes typically feed on other sugars only when glucose is not present. The regulatory mechanism by which the expression of genes required for the utilization of secondary carbon sources is prevented in the presence of a preferred substrate is known as carbon catabolite repression (CCR).[4] CCR enables microbes to increase their fitness by optimizing growth rates in natural environments that provide complex mixtures of nutrients. On the other hand, in industrial processes such as biofuel production, CCR is one of the barriers to the increased yield of fermentation products.[5] During *E. coli* glucose-lactose diauxie, the presence of glucose represses the *lac* operon, a set of genes coding for the *lac* permease and *β*-galactosidase which are required for lactose uptake and lactose hydrolysis to catabolizable glucose and galactose subunits, respectively.[6]

Optical density (OD) measurements are commonly used to monitor diauxic growth.[1,2,7] They rely on the principle that transmitted light is lost because of scattering by the microbial culture. The OD is thus an indirect measure of the concentration of microbial cells. OD measurements are simple, but they suffer from interference because they cannot distinguish living cell from debris, dead cells, or precipitates. The diauxic lag phase between the consumption of the first nutrient and the second often gives a distinct plateau in OD values due to the temporary halt in growth. However, this classic picture of diauxic growth intermittent with a lag phase is not always the case. Some strains of budding yeast when presented with a mixture of glucose and galactose exhibit a very brief diauxic lag phase and little change in growth rates between glucose and galactose consumption.[8] Furthermore, although glucose sits at the top of the sugar hierarchy for *E. coli* and is frequently consumed first, mixed nonglucose sugars may exhibit simultaneous metabolism rather than sequential.[9] OD

Received: July 19, 2019
Accepted: September 16, 2019
Published: September 16, 2019

DOI: 10.1021/acs.analchem.9b03284
Anal. Chem. 2019, 91, 13096−13104

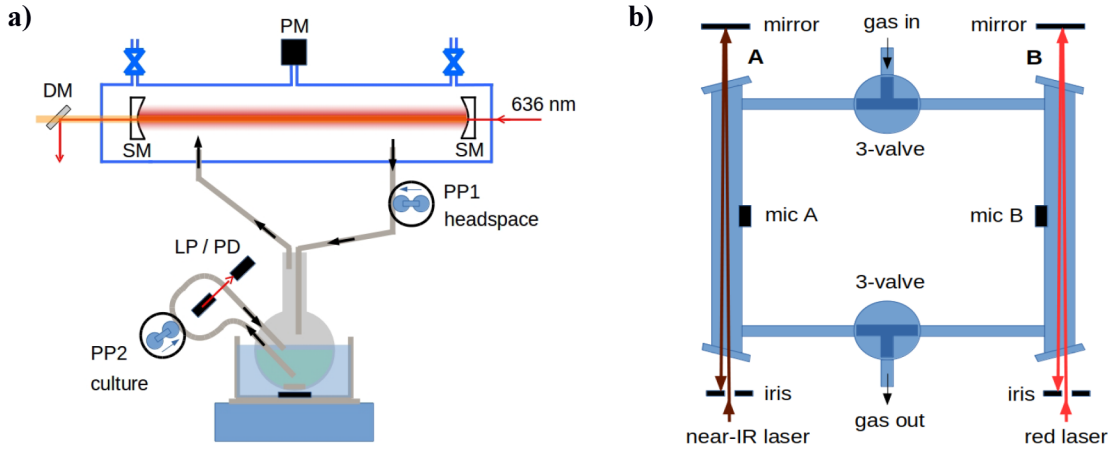

Figure 1. Schemes of the experimental setups. See the main text for details. (a) CERS with bacterial suspension attached and peristaltic pumps cycling the headspace for CERS and the culture solution for OD measurements. (b) Differential Helmholtz resonator.

measurements alone cannot provide sufficient information for mixed sugar metabolism. Another common method for monitoring diauxic growth is sampling the microbial culture for high-performance liquid chromatography analysis to determine changes in mixed sugar concentrations during metabolic activity.[10−12] Analytical methods that require sampling are not ideal because they consume the analyte and require extra considerations to prevent contamination of the system.

The gas composition is another process parameter frequently monitored online in bioreactors. O_2 and CO_2 are two key gases to consider.[13] O_2 availability is a key parameter for aerobic bioprocesses as well as anaerobic systems that are sensitive to disruption by O_2, such as the production of biohydrogen. CO_2 is a key byproduct of both aerobic respiration and fermentation and can be monitored to closely follow these processes. Dissolved gases can be monitored by gas-sensitive electrode-based sensors, some of which have the advantage of not consuming the analyte. However, most sensors are invasive because they must be submerged in the microbial culture and often have a limited lifespan under the operating conditions of the bioreactor as a result of poisoning. Online, solution-based sensors create challenges such as the requirement for including an additional port on the bioreactor, an increased risk of contamination, and the challenges associated with sterilization and needing to frequently calibrate the sensor, which is often impossible without process contamination. Disadvantages also include interference with other components, aging, temperature dependence, and long response and settlement times. The measurement of partial pressures in the effluent headspace gases can give a good approximation of dissolved gases via Henry's law and eliminates the need to use invasive devices. Gas chromatography (GC) and mass spectrometry (MS) are two common methods of gas-phase analysis. However, both techniques require sampling, are expensive, require frequent calibration, and have limitations, including difficulties detecting certain components. Also, chromatographic techniques rely upon the spatial separation of the compounds that are being quantified and so are only of use on a noncontinual basis.[14] Spectroscopic methods for gas-phase analysis offer numerous benefits including high precision and accuracy, no sampling necessary, and the ability to perform noninvasive real-time measurements. Detection in the near-IR has the advantage of low-cost light sources and detectors; the sensitivity, however, suffers from low absorption cross sections. In addition, relevant homonuclear molecules including O_2 cannot be observed by IR absorption because of the unfavorable selection rules. Molecular O_2 has two main absorption bands in its UV−vis spectrum: one deep in the UV at 145 nm and the other at 760 nm.[15,16] O_2 detection at 145 nm faces interference by water vapor and CO_2, and the weak absorption lines at 760 nm typically provide detection limits that are of little practical use. Raman spectroscopy, in contrast, can detect homonuclear molecules, but it has very low sensitivity. Both near-IR absorption and Raman spectroscopy need special enhancement techniques to be useful in gas-phase analysis.

Recently, two new techniques were introduced for sensitive and selective trace gas detection: near-IR absorption enhanced by photoacoustic detection in a differential Helmholtz resonator (DHR)[17−20] and cavity-enhanced Raman spectroscopy (CERS).[21−25] In this article, we apply these techniques to the study of the metabolic growth of microbes and compare their performance and suitability for applications in the biosciences and biotechnology. We demonstrate that both spectroscopic techniques can clearly and unambiguously distinguish all of the main phases of bacterial growth, can monitor the consumption of a mixed organic feedstock using ^{13}C isotopic labeling of sugars, and can be employed to establish whether the various components are sequentially or simultaneously metabolized.

EXPERIMENTAL SECTION

The headspace above bacterial cultures is analyzed by Raman (CERS) or diode laser photoacoustic (DHR) spectroscopy. The CERS setup has been described in detail before.[21,23,24] Here, we provide a brief outline and describe some modifications and improvements. A higher-power diode is employed (Opnext HL63133DG), lasing at 636.7 nm. At full driving current, the laser can provide up to 170 mW continuous wave (cw) power, but in CERS, it is operated at a reduced power of 40 mW to facilitate single mode operation. The laser output is coupled via a short-pass filter and two Faraday isolators into an optical cavity composed of two highly reflective mirrors (Newport SuperMirrors, $R > 99.99\%$, SM in Figure 1a). To simplify the setup, no anamorphic prism pair or mode-matching lens is used; mode matching/focusing into the cavity is achieved by optimizing the distance of the collimating

DOI: 10.1021/acs.analchem.9b03284
Anal. Chem. 2019, 91, 13096−13104

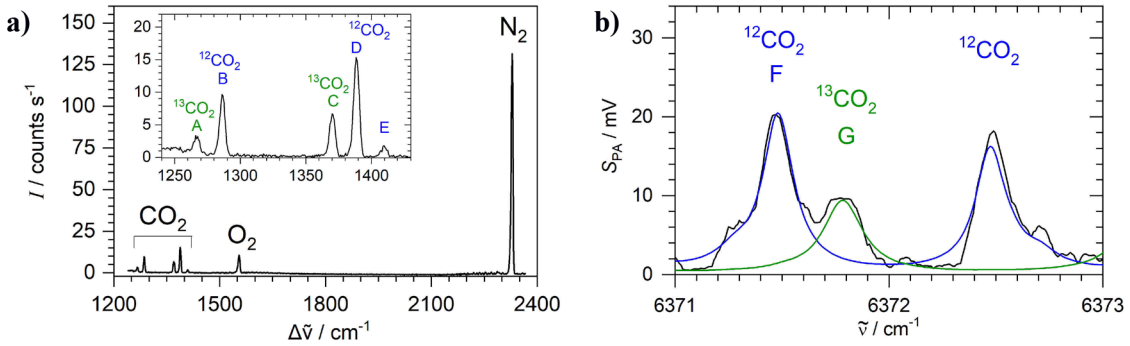

Figure 2. Spectral signatures used to identify $^{12}CO_2$ and $^{13}CO_2$ in the headspace of the mixed sugar aerobic metabolism (^{13}C-glucose, ^{12}C-lactose) of *E. coli*. (a) CERS Raman spectrum of 800 mbar N_2, 65 mbar O_2, 73 mbar $^{12}CO_2$, and 31 mbar $^{13}CO_2$. (b) DHR absorption spectrum (black) of 6.5 mbar $^{12}CO_2$ and 5.0 mbar $^{13}CO_2$. In blue and green are HITRAN data for $^{12}CO_2$ and $^{13}CO_2$, respectively.

lens of the diode. If the laser wavelength matches the cavity length, then an optical resonance builds up laser power inside the cavity by up to 3 orders of magnitude, enhancing the Raman signals (CERS). After the cavity, a dichroic mirror DM separates excitation light from Raman signals which are coupled into a fiber and transferred to the spectrometer (Shamrock SR-750-A with an Andor iVac DR32400 camera at −60 °C). The 600 lines/mm grating provides a 1200 cm^{-1} spectral range at 5 cm^{-1} resolution which covers CO_2, O_2, and N_2 Raman peaks and can easily resolve $^{12}CO_2$ and $^{13}CO_2$ (Figure 2a). Part of the laser light is diverted back to the diode for optical feedback, locking the laser to the cavity. The diode injection current is modulated around one cavity mode; in each cycle, the wavelength changes until it is self-locking by optical feedback to a longitudinal cavity mode. In a simplification of the setup, no attempts are made to actively stabilize the laser because the optical self-locking is strong enough to keep accidental resonances at duty cycles between 50 and 80%. To normalize Raman signals, the N_2 peak of air can be used because, in the closed system, N_2 is not consumed or produced by bacterial metabolism. Alternatively, Si peaks presumably from the SM mirror and glass substrates can also be used for convenient in situ calibration. The Raman intensity is converted to partial pressure using tabulated integrated peak areas.[23]

The DHR setup has been described in detail in a previous publication.[20] In short, optical absorption in a differential Helmholtz resonator (Figure 1b) creates sound waves (the photoacoustic effect) in chambers A and B, which are 180° out of phase. Acoustic noise, including flow noise, will be mostly in-phase. Differential detection of the sound in A minus B therefore doubles the signals and effectively cancels noise. Two temperature-tuned distributed feedback (DFB) diode lasers are used: a near-IR laser (Mitsubishi FU-650SDF, amplified to 30 mW in a booster optical amplifier Thorlabs S9FC1004P) to detect CO_2 near 1.57 μm and a red laser (35 mW, Eagleyard EYP-DFB-0764) to detect O_2 near 764 nm. To simplify the setup, the near-IR laser is directed through one compartment (A) and the red laser is directed through the other (B) (Figure 1b). In a typical experiment, CO_2 is first measured by scanning the near-IR laser; next, O_2 is measured by scanning the red laser.[20] Both lasers are modulated by their injection current at the acoustic resonance frequency with a square wave at the 50% duty cycle. The near-IR spectrum allows the distinction of $^{12}CO_2$ and $^{13}CO_2$ (Figure 2b). The photoacoustic signal is converted to partial pressure using our previous calibration and HITRAN absorption cross sections.[20,26]

The molarity of a dissolved gas can be calculated from its partial pressure using Henry's law.[27] A small proportion of dissolved CO_2 will react with water to form carbonic acid, which will be at equilibrium with bicarbonate and carbonate ions, depending on the pH. With a typical acidic pH below 5 at the end of an experiment, less than 1% of the dissolved CO_2 will be lost to carbonic acid and carbonates.

For each measurement, 50 mL of sterile LB (lysogeny broth, a nutrient-rich growth medium) was inoculated with a single colony of *E. coli* (wild type, strain K-12 MG1655) and incubated for 5 h at 37 °C to grow to typically 1.0 OD_{600} (OD at 600 nm in a 1 cm cuvette). One milliliter of the suspension was then centrifuged to remove the LB medium and resuspended in 250 mL of fresh, sterile M9 (a minimal, defined medium containing only essential salts and vitamins) or LB solution. The medium was supplemented with D-glucose and/or D-lactose (puriss. p.a., Sigma-Aldrich). For isotope-labeling experiments, fully ^{13}C-substituted glucose (U-13C6, 99% CLM-1396, CK isotopes) was used. In mixed sugar experiments, we used larger concentrations of lactose compared to glucose to show the preference for glucose more clearly. This is in line with most previous studies of glucose−lactose diauxie which have used a lactose concentration that was up to 1 order of magnitude greater than the glucose concentration.[28−30] The glucose concentration was selected to ensure that oxygen was not depleted so that the shift to lactose metabolism could occur while still producing appreciable CO_2 from glucose metabolism.

The bacterial batch culture in a 500 mL flask was kept at 37 °C in a thermostated water bath under constant stirring. The headspace was circulated via a peristaltic pump (3 L/h) through the spectroscopic cell in a closed, vacuum-tight system (Figure 1a). The total headspace gas volume is 720 mL in the CERS system and 510 mL in the DHR system. The transfer tubes and cells were kept at ca. 45 °C using a heating wire to avoid water condensation. This was particularly important and effective for avoiding condensation on the high-performance cavity mirrors, which would spoil their reflectivity. In control experiments, we measured the appearance time from the suspension flask to the spectroscopic measurement cell to be less than 5 min.[20,24] To characterize bacterial growth by measuring the OD in situ, another peristaltic pump circulated part of the suspension through a 1 cm glass cuvette, through which a red laser pointer (1 mW, 650 nm) was shining (Figure

DOI: 10.1021/acs.analchem.9b03284
Anal. Chem. 2019, 91, 13096−13104

1a). After calibration with a UV−vis spectrometer, the transmitted intensity as observed by a photodiode is converted to OD_{600}. At the end of an experiment and after exhausting the oxygen supply, the increase in cell density is characterized by $OD_{600} \approx 1.5-2.0$. The final pH of the solution was typically 4.5 to 5.0 because of organic acids generated during the metabolism. For comparison, fresh LB has pH ≈ 6.8, and fresh M9 has pH ≈ 6.9. At the beginning, the cellular material within the 250 mL suspension has a typical dry weight of 0.2 mg, which by the end of a typical experiment increases to 60 mg, reflecting bacterial growth. All experiments were repeated at least three times, exhibiting essentially the same behavior.

RESULTS AND DISCUSSION

***E. coli* Metabolism in LB or M9 Supplemented with Glucose or Lactose.** In the first set of experiments, we studied the oxygen-limited growth of *E. coli* batch cultures in LB or M9 medium supplemented with a single sugar, glucose or lactose. Figure 3 shows typical time-dependent partial pressures of O_2 and CO_2 as measured by CERS with simultaneous OD measurements for *E. coli* in LB supplemented with 20 mM glucose. Also included in Figure 3 (middle panel) is the total pressure $p'_{total} = p_{O_2} + p_{CO_2} + p_{N_2}$ and the respiratory quotient (RQ), the ratio of CO_2 produced to O_2 consumed, where CO_2 is corrected to account for the approximately 18% of dissolved CO_2 according to Henry's law.[27] After a lag phase of approximately 2 h (A in Figure 3), oxygen consumption and CO_2 production begin, indicating the onset of exponential bacterial growth (B in Figure 3). This is also indicated by the increase in OD up to a peak value of about 1.5 in Figure 3, lower panel. After around 5.5 h, the OD plateaus, indicating the onset of the stationary phase (C in Figure 3). The living bacteria in the stationary population still consume O_2 and produce CO_2. During exponential phase B and stationary phase C, the oxygen uptake rate is constant, as indicated by the almost perfect exponential decay fit of oxygen partial pressure in Figure 3, with a rate constant of $k = 0.189$ h^{-1} or a half-life of $t_{1/2} = 3.67$ h. These results are confirmed in three repeated experiments which show a lag phase between 1.5 and 2 h, the onset of the stationary phase between 5 and 6 h, and an oxygen uptake rate within 0.15−0.19 h^{-1}.

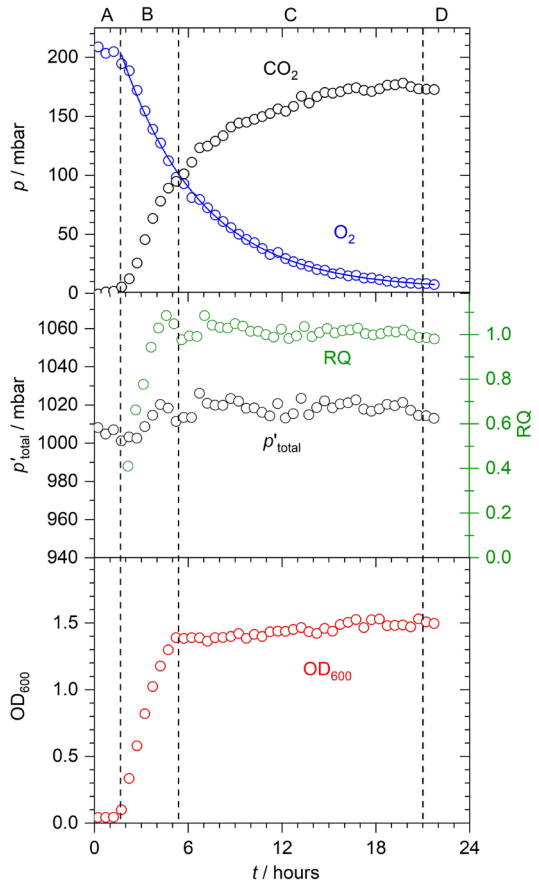

Figure 3. CERS measurement of the headspace in the aerobic *E. coli* metabolism of unlabeled glucose (20 mM) in a rich LB medium. A−D denote different phases of bacterial growth: lag phase, exponential growth, stationary phase, and the end of aerobic respiration, respectively. (Upper panel) Partial pressures of O_2 and CO_2, including an exponential decay fit of p_{O_2}. (Middle panel) p'_{total} (total of N_2, O_2, and corrected CO_2 pressures) and respiratory quotient RQ (ratio of CO_2 produced to O_2 consumed). (Lower panel) Simultaneous OD measurements of the bacterial culture.

During cellular energy production by aerobic respiration with glucose as a carbon source, the sugar is oxidized to CO_2 and H_2O. Full conversion is described by the stoichiometry of eq 1

$$C_6H_{12}O_6 + 6O_2 = 6CO_2 + 6H_2O \quad (1)$$

so that for each unit of O_2 consumed, one unit of CO_2 is formed. For carbohydrates, the respiratory quotient RQ is therefore typically about 1.0. Like OD measurements, the RQ can be used to distinguish between exponential phase B and stationary phase C as shown in Figure 3, middle panel, where a constant RQ of about 1.0 (within 2% in the three repeat experiments) is reached during stationary growth. The 1:1 ratio between O_2 consumed and CO_2 produced can also be observed in the constant total pressure during stationary growth in Figure 3, middle panel. A typical *E. coli* cell contains approximately 50% carbon by dry mass.[31] Because sugars are primarily used for energy production, the carbon source for biosynthesis and growth in the LB medium originates from the tryptone and yeast extract (see also ref 32). *E. coli* has several oligopeptide permeases and peptidases enabling it to recover free catabolizable amino acids from tryptone and yeast extract.[33] The available oxygen in 1 atm of air in the 720 mL headspace of the CERS experiment corresponds to 6 mmol, and the 20 mM glucose in the 250 mL suspension corresponds to 5 mmol of glucose. According to eq 1, there is therefore an excess of glucose in the experiment and the bacteria are limited by the oxygen available, hence the decrease of O_2 partial pressure down to essentially 0 in the closed system. After about 21 h, all available oxygen in the closed system has been consumed, and aerobic respiration terminates (D in Figure 3). *E. coli* is a facultative anaerobe, meaning that upon shifting to anaerobic conditions, the microbes may adapt to the new environment and resume metabolism by the anaerobic fermentation of excess glucose. However, we do not see any evidence of further microbial activity such as resuming CO_2 production. The partial pressure of CO_2 was monitored for up to 3 days (not shown in Figure 3), during which time CO_2 did not increase but rather gradually decreased to a constant value of around 145 mbar. This decrease was not due to a leak because no increase in O_2 was observed. One possible explanation might be provided by the slow conversion of

DOI: 10.1021/acs.analchem.9b03284
Anal. Chem. 2019, 91, 13096−13104

dissolved CO_2 to carbonic acid. Although OD measurements are convenient for indicating the stage of bacterial growth (i.e., lag, exponential, and stationary phases), the OD cannot determine the point of oxygen depletion because there is no change in OD between phases C and D. The OD measurements also do not indicate that CO_2 production, and thus the overall metabolic activity of *E. coli*, halts under the anaerobic conditions of phase D. For a full characterization of bacterial growth in changing environments, OD measurements require a complementary method to provide information on changes such as the shift from aerobic to anaerobic conditions.

To make sure that in the isotopically labeled mixed sugar metabolism experiments all CO_2 observed was coming from the sugars and not from the medium, we also performed experiments in an M9 minimal medium. Figure 4 shows a

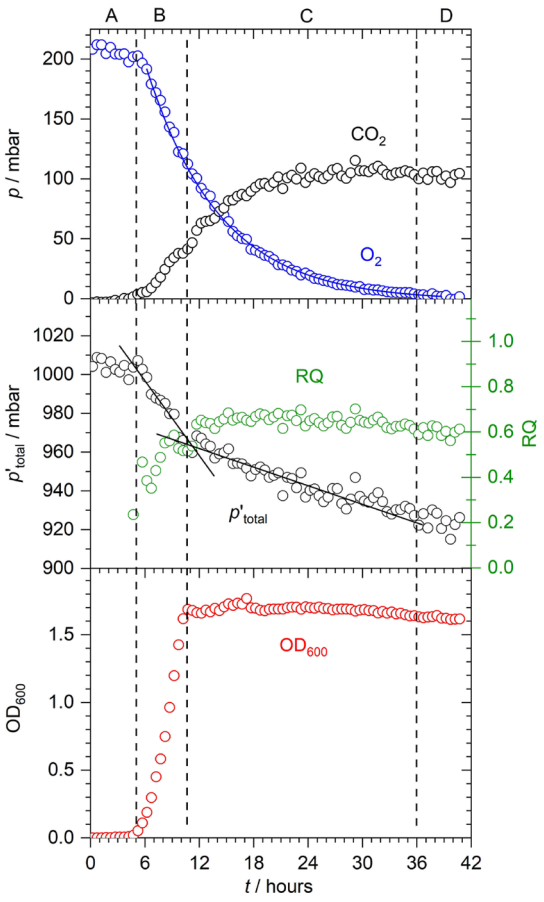

Figure 4. As in Figure 3 but now monitoring the aerobic *E. coli* metabolism of unlabeled glucose (20 mM) in M9 minimal medium instead of LB medium.

typical time-dependent CERS measurement of oxygen and CO_2 partial pressures with simultaneous OD measurements for the metabolism of *E. coli* in M9 supplemented with 20 mM glucose. As before, the four different phases A to D can be clearly distinguished by the gas analysis while OD is unable to distinguish the stationary phase C from the end of aerobic respiration D. With about 5 h, the lag phase is much longer compared to that in the LB medium. The oxygen uptake rate is constant, as indicated by the almost perfect exponential decay fit of oxygen partial pressure in Figure 4. The decay extends from the exponential phase to the stationary phase with a rate constant of $k = 0.134\ h^{-1}$ or a half-life of $t_{1/2} = 5.18$ h, which is much slower than in LB. The longer lag phase and the slower oxygen uptake and growth reflect the limitations of the minimal medium compared to the rich LB medium. Similar results were found in three repeat experiments which show a lag phase of between 4 and 7 h, the onset of stationary phase between 10 and 13 h, and oxygen uptake rates of between 0.13 and 0.15 h^{-1}.

A very distinct different behavior is exhibited in terms of the total yield of CO_2. There is no 1:1 relationship between oxygen consumed and CO_2 being formed, but rather a considerable amount of CO_2 is missing. The RQ during stationary phase growth of about 0.6 (within 2% in the three repeat experiments) indicates that around 40% of CO_2 is missing. This is even clearer in the plot of the total pressure $p_{O_2} + p_{CO_2} + p_{N_2}$ (with a correction for dissolved CO_2), also in the middle panel of Figure 4. The "missing" CO_2 is not due to leaching some dissolved CO_2 via carbonic acid into bicarbonate and carbonate ions as determined in a test experiment, in which acidifying by injecting HCl into the suspension at the end of growth did not release any noticeable CO_2 over an extended period of time. The imbalance between O_2 consumption and CO_2 production in the M9 medium is due to some glucose not being fully oxidized to CO_2 because it is the only available carbon source for biomass synthesis, while O_2 is still consumed. Tryptone and yeast extract provide amino acids for growth in LB medium, but in minimal medium, *E. coli* must synthesize amino acids, nucleobases, and other biomolecules from glucose. In minimal media, *E. coli* has been found to accumulate a large amount of enzymes, which are virtually absent when grown in LB medium and catalyze the formation of amino acids from glucose, ammonia, and sulfate.[34] Some formulations of minimal media incorporate casamino acids for biomass synthesis so that sugars are not utilized as building blocks. We did not incorporate casamino acids into the M9 medium to be certain that the only available carbon sources for CO_2 production were the supplemented sugars. The need to synthesize essential precursor molecules in M9 medium also contributes to the longer lag phase and slower growth rate. It can be seen from the plot of the total pressure that the rate of decrease is much higher during exponential growth phase B than during stationary phase C. This is consistent with a more significant imbalance between CO_2 and O_2 and a higher requirement for carbon for growth during the exponential phase. About 80 mbar of CO_2 is missing at the end of the experiment, which corresponds to approximately 2.5 mmol of carbon atoms. The dry weight of bacteria at the end is about 60 mg. Assuming that about 50% of this is carbon, the bacteria contain about 2.5 mmol of carbon atoms in total, in agreement with the missing CO_2.

Experiments were repeated in M9 supplemented with lactose. Figure 5 shows typical time-dependent traces for the aerobic metabolism of *E. coli* in M9 supplemented with 20 mM lactose, as measured by CERS with simultaneous OD measurements. The results are very similar to M9 supplemented with glucose with a similar lag phase. The exponential decay of oxygen is characterized by an uptake rate of $k = 0.155\ h^{-1}$ (half-life $t_{1/2} = 4.47$ h) with a range of 0.15−0.17 h^{-1} in the three repeats. This is somewhat faster compared to glucose but probably not different enough to allow the distinction between lactose and glucose metabolism just from a measurement of the uptake rate. Lactose ($C_{12}H_{22}O_{11}$) is a disaccharide derived from the condensation of glucose and galactose. At complete

DOI: 10.1021/acs.analchem.9b03284
Anal. Chem. 2019, 91, 13096−13104

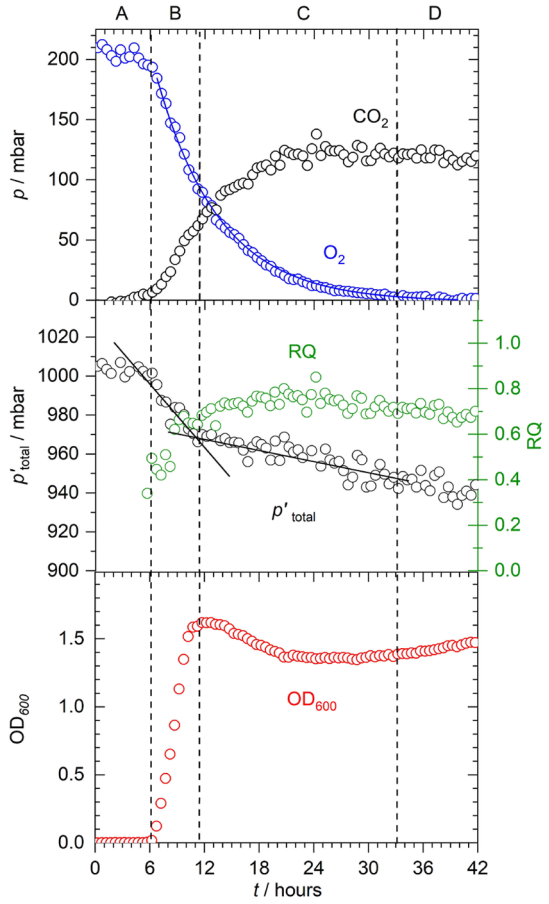

Figure 5. As in Figures 3 and 4, but now monitoring the aerobic *E. coli* metabolism of unlabeled lactose (20 mM) in a minimal M9 medium.

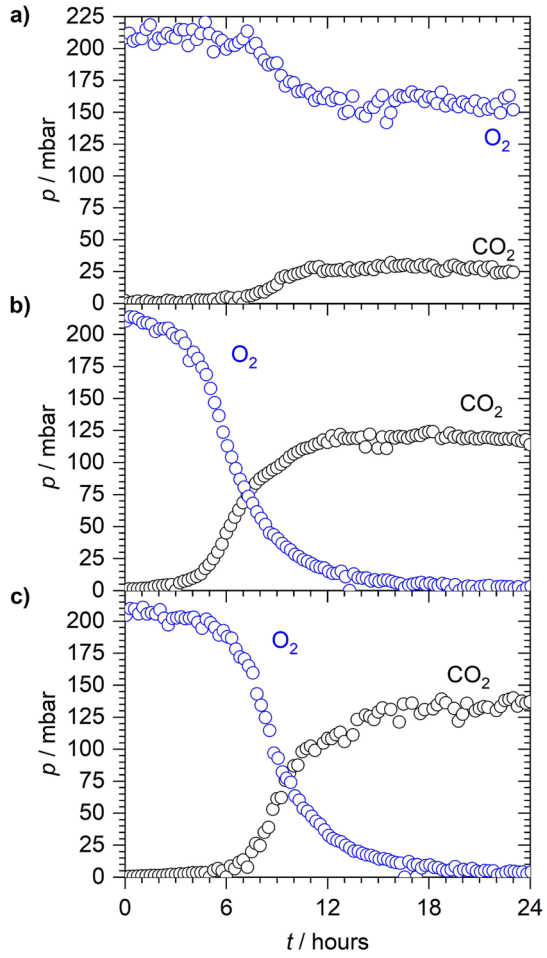

Figure 6. DHR measurement of the headspace in the aerobic *E. coli* metabolism of unlabeled sugars in a minimal M9 medium (a) supplemented with 2.5 mM glucose, (b) supplemented with 10 mM lactose, and (c) supplemented with 2.5 mM glucose and 10 mM lactose.

conversion to CO_2 and H_2O, there is again a 1:1 relationship between oxygen consumed and CO_2 being formed. In M9, however, a considerable amount of CO_2 is missing as in the previous example of glucose in M9. As before, CO_2 is missing because the bacteria need a carbon source for their growth. Because the minimal medium contains no other source of organic carbon, the bacteria must utilize lactose. A noticeable difference concerns the behavior of the OD curve. As before, the lag phase and exponential growth can be easily seen in the OD curve. In the stationary phase, however, the OD does not remain constant but first declines a little before increasing again around the point where aerobic respiration terminates, continuing to rise outside the range displayed in Figure 5. The reason for this behavior is unclear at present; it might be related to dead cells breaking up, possibly releasing slightly colored compounds which absorb red light, in addition to scattering losses. In any case, it shows that an OD measurement is a rather indirect determination of cell density and therefore can suffer from interferences not directly related to the density of living cells.

Aerobic Mixed Sugar Metabolism of *E. coli*. Experiments were also done using DHR to characterize the metabolism. In the DHR experiments, we used a lower sugar concentration (10 mM), and because of the lower headspace volume, there is also less oxygen available in the closed system. Typical examples of DHR measurements with unlabeled sugars are shown in Figure 6. The same qualitative behavior as in the CERS measurement was found, with the exception of the oxygen uptake rate being faster with typically k = 0.20−0.25 h^{-1} within our repeats. The faster kinetics must be related to the difference in the experimental conditions such as more efficient O_2 mass transfer to the solution or differences in the sugar concentrations. Figure 6 shows that without isotope labeling it is not really possible to distinguish the metabolism of different sugars from the measurements of O_2 and CO_2 partial pressures. In Figure 6a, M9 was supplemented with 2.5 mM glucose; in this experiment, the glucose is limiting, not the oxygen. Figure 6b shows the metabolism of 10 mM lactose, and Figure 6c shows the mixed sugar metabolism of 2.5 mM glucose *and* 10 mM lactose in M9. Even on close inspection of Figure 6c, no classic diauxic shift lag phase is apparent, which would indicate the shift from one sugar to the other; in fact, it would be even unclear whether glucose or lactose is first metabolized or both are metabolized simultaneously.

The power of spectroscopic detection, however, is the possibility to distinguish isotopes which allow the ^{13}C labeling of sugars and the detection of $^{13}CO_2$ in the headspace. Using spectroscopy, this can be easily quantified and distinguished from $^{12}CO_2$ derived from nonlabeled organic compounds. This principle is demonstrated in Figure 7, showing an experiment with 2.5 mM ^{13}C-glucose and 10 mM ^{12}C-lactose in M9 as measured by DHR, and in Figure 8, showing an experiment

DOI: 10.1021/acs.analchem.9b03284
Anal. Chem. 2019, 91, 13096−13104

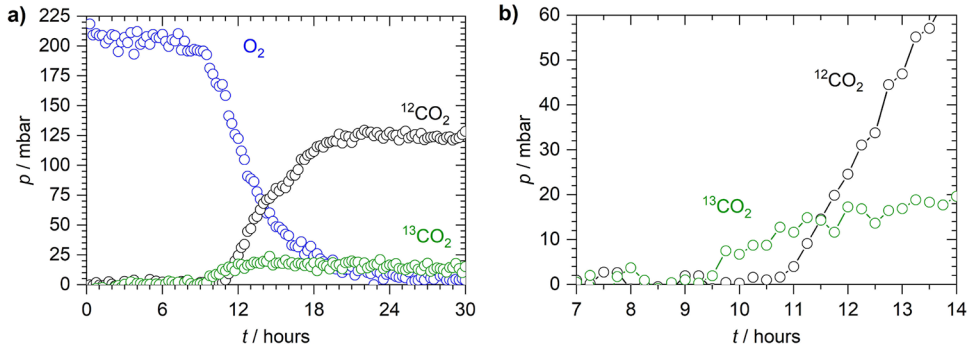

Figure 7. Monitoring mixed sugar metabolism of *E. coli* using DHR photoacoustic spectroscopy with isotopic labeling (2.5 mM ^{13}C-glucose and 10 mM ^{12}C-lactose in M9). (a) Overview. (b) Detail.

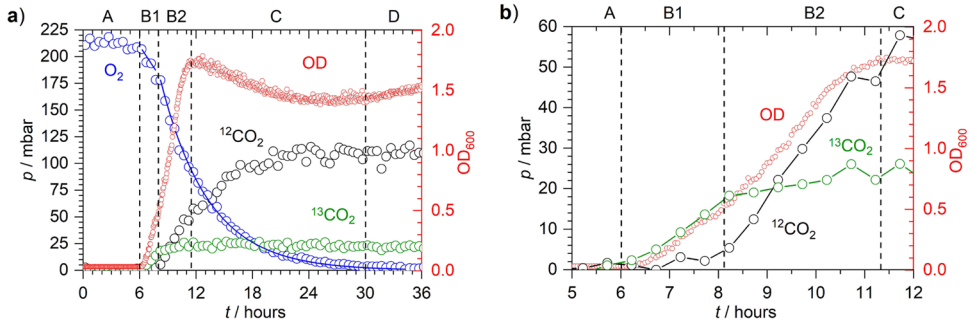

Figure 8. Monitoring mixed sugar metabolism of *E. coli* using CERS spectroscopy with isotopic labeling (3 mM ^{13}C-glucose and 20 mM ^{12}C-lactose in M9), including an exponential decay fit of p_{O_2} and OD measurements of the culture solution. Different phases of bacterial growth: lag phase (A), exponential growth (B1 glucose, B2 lactose), stationary phase (C), and end of aerobic respiration (D). (a) Overview. (b) Detail.

with 3 mM ^{13}C-glucose and 20 mM ^{12}C-lactose in M9 as measured by CERS. Both DHR and CERS are capable of distinguishing $^{13}CO_2$ arising first from the ^{13}C-labeled glucose and $^{12}CO_2$ arising from the unlabeled lactose. We discuss the mixed sugar metabolism of *E. coli* using the CERS experiment in Figure 8 as an example; the DHR results and all repeats (at least in triplicate) have essentially the same qualitative and quantitative behavior. As before, there is a lag phase of about 6 h (A in Figure 8) after which exponential growth sets in (B in Figure 8). Exponential growth is characterized by an increase in the OD up to its peak value of about 1.8. After ca. 11.5 h, the OD remains more or less stationary, indicating the stationary phase (C in Figure 8). During the exponential growth and stationary phase, oxygen is continuously consumed and CO_2 formed until after about 30 h all oxygen is consumed, indicating the end of aerobic respiration (D in Figure 8). The OD during phases C and D does not remain constant but declines first and then rises again; this behavior seems to be typical for lactose metabolism and was discussed before. As before, there is some CO_2 missing in the total balance, which is attributed to incomplete conversion of the sugars to CO_2 because M9 does not contain an alternative carbon source for bacterial growth.

During the exponential growth phase, there is clearly a shift from glucose metabolism (B1 in Figure 8) to lactose metabolism (B2). As expected, glucose is metabolized first. When glucose is nearly exhausted, lactose metabolism takes over, without any apparent diauxic lag phase. In addition, there is possibly some overlap between glucose and lactose metabolism. Similar observations were made by Wang et al. in which *Saccharomyces cerevisiae* natural isolates growing in mixtures of glucose and galactose would switch to metabolizing both sugars before all glucose was exhausted.[35] They state that classic diauxic growth with a distinct lag phase is one extreme on a continuum of growth strategies determined by a cost–benefit trade-off. In the literature, under conditions similar to those in our experiment, diauxic lag phases typically of up to 1 h have been reported for the diauxic shift from glucose to lactose in *E. coli*, often including OD measurements which showed an increase during glucose metabolism and then a lag phase (stationary OD), followed by a further increase attributed to lactose metabolism.[1,2,36] In our experiments, no prolonged diauxic lag is apparent in the oxygen consumption/CO_2 production or in the OD measurements (Figure 8b). All of our measurements have a smooth transition from B1 (glucose metabolism) to B2 (lactose metabolism). Only the p_{O_2} shows perhaps a slightly different decay slope in B1 compared to that in B2 (Figure 8a, solid blue line). Diauxic growth is not always made clear by a prolonged lag phase. Chu and Barnes proposed a hypothesis that the length of the diauxic lag phase depends on the characteristics of the environment.[37] Bacteria growing in rapidly changing environments need to be able to rapidly adapt between two sugars. Our environment is distinct from the majority of previous work studying diauxic shifts because it is oxygen-limited, and the effects of rapidly depleted oxygen levels on the glucose–lactose diauxic growth of *E. coli* are as of yet unknown.

In conclusion, without the spectroscopic distinction of the ^{13}C-labeled and unlabeled sugars, no preference or diauxic shifts of metabolism would be apparent in our CO_2/O_2 or OD measurements. Despite their widespread use, OD measurements are a very indirect method of characterizing bacterial growth and phases. However, they are prone to interference

DOI: 10.1021/acs.analchem.9b03284
Anal. Chem. 2019, 91, 13096−13104

and should be used only in combination with more advanced techniques to supplement more specific measurements such as the spectroscopic measurements in the present study.

CONCLUSIONS

Measuring the headspace above bacterial suspensions by spectroscopy to characterize bacterial growth and metabolism has many advantages compared to more conventional techniques. It is nonintrusive, it does not require sampling and thus can be applied to closed systems easily, and it is very sensitive and highly selective because of the spectroscopic fingerprint of headspace gases. The high selectivity allows isotopic distinction, which enables isotopic labeling studies. In this article, we have introduced two powerful new techniques for headspace monitoring: photoacoustic detection in a differential Helmholtz resonator (DHR) and Raman spectroscopy enhanced in an optical cavity (CERS). Both techniques have been shown to be able to monitor O_2 and CO_2 and its isotopomers with excellent sensitivity and time resolution. Compared to DHR, CERS has the advantage of easier calibration due to the availability of internal standards (N_2 or Si peaks). Without further modifications, the CERS method can also detect other important gases in the metabolism of bacteria, such as H_2, H_2S, or N_2. DHR has the advantage of a much simpler setup and being even more cost-effective. The technique can measure O_2, CO_2, and H_2S with high sensitivity and selectivity; extension to the detection of other molecules would require different diode laser sources, however.

OD measurements are a standard, widely used technique to characterize bacterial growth. We have discussed and shown some of its shortcomings if used on its own without supporting complementary measurements. OD measurements are an indirect indicator of bacterial growth. They suffer from interference, and they cannot distinguish living cells from dead cells and debris. OD measurements can therefore not provide sufficient information once the OD becomes constant during the stationary phase of bacterial growth. They also cannot distinguish diauxic growth without a diauxic lag phase present. The spectroscopic measurements, however, can clearly and unambiguously distinguish the different stages of bacterial growth characterizing the growth phases in the different media studied, LB and M9. OD measurements can supplement these measurements, but they are not necessary. We have demonstrated how ^{13}C isotopic labeling of sugars in the spectroscopic detection allows the study of bacterial mixed sugar metabolism to establish whether sugars are sequentially or simultaneously metabolized. For *E. coli*, we have characterized the shift from glucose to lactose metabolism without a classic diauxic lag phase in-between, under oxygen-limited conditions.

DHR and CERS have been proven to be cost-effective, highly specific analytical tools in the biosciences and in biotechnology, complementing and superseding existing conventional techniques. They also provide new capabilities for mechanistic investigations, in particular due to the possibility to use isotopic labeling easily. In the future, we plan to apply these techniques to further mechanistic studies of bacterial metabolism, monitoring of continuously operating systems, and anaerobic bioprocesses.

AUTHOR INFORMATION

Corresponding Author

*E-mail: M.Hippler@sheffield.ac.uk.

ORCID

Michael Hippler: 0000-0002-3956-3922

Notes

The authors declare no competing financial interest.

ACKNOWLEDGMENTS

We are grateful to Prof. J. Green, Prof. R. K. Poole, and Dr. J. Reid for help and discussions. We acknowledge the University of Sheffield, the NERC research council (CERS setup, grant NE/I000844/1), the EPSRC (DTP scholarship to G.D.M.), and the Ministry of Education of Saudi Arabia for the financial support of our research.

REFERENCES

(1) Monod, J. *Recherches sur la croissance des cultures bactériennes*. Thesis, Université de Paris, 1941.
(2) Monod, J. *Annu. Rev. Microbiol.* **1949**, *3*, 371−394.
(3) Santillán, M.; Mackey, M. C. *J. R. Soc., Interface* **2008**, *5* (Suppl. 1), S29−S39.
(4) Görke, B.; Stülke, J. *Nat. Rev. Microbiol.* **2008**, *6*, 613−624.
(5) Dien, B. S.; Nichols, N. N.; Bothast, R. J. *J. Ind. Microbiol. Biotechnol.* **2002**, *29*, 221−227.
(6) Ullmann, A. Escherichia coli Lactose Operon. *Encyclopedia of Life Sciences (ELS)*. Wiley & Sons, Ltd: Chichester, U.K., 2009.
(7) Solopova, A.; van Gestel, J.; Weissing, F. J.; Bachmann, H.; Teusink, B.; Kok, J.; Kuipers, O. P. *Proc. Natl. Acad. Sci. U. S. A.* **2014**, *111*, 7427−7432.
(8) Siegal, M. L. *PLoS Biol.* **2015**, *13*, e1002068.
(9) Aidelberg, G.; Towbin, B. D.; Rothschild, D.; Dekel, E.; Bren, A.; Alon, U. *BMC Syst. Biol.* **2014**, *8*, 133.
(10) Joshua, C. J.; Dahl, R.; Benke, P. I.; Keasling, J. D. *J. Bacteriol.* **2011**, *193*, 1293−1301.
(11) Desai, T. A.; Rao, C. V. *Appl. Environ. Microbiol.* **2010**, *76*, 1524−1532.
(12) Ammar, E. M.; Wang, X.; Rao, C. V. *Sci. Rep.* **2018**, *8*, 609.
(13) Holzberg, T. R.; Watson, V.; Brown, S.; Andar, A.; Ge, X.; Kostov, Y.; Tolosa, L.; Rao, G. *Curr. Opin. Chem. Eng.* **2018**, *22*, 115−127.
(14) Dixon, N. M.; Kell, D. B. *J. Microbiol. Methods* **1989**, *10*, 155−176.
(15) Arnoudse, P. B.; Pardue, H. L. *Anal. Chem.* **1992**, *64*, 200−204.
(16) Gianfrani, L.; Sasso, A.; Tino, G. M. *Sens. Actuators, B* **1997**, *39*, 283−285.
(17) Busse, G.; Herboeck, D. *Appl. Opt.* **1979**, *18*, 3959−3961.
(18) Zeninari, V.; Courtois, D.; Parvitte, B.; Kapitanov, V. A.; Ponomarev, Y. N. *Infrared Phys. Technol.* **2003**, *44*, 253.
(19) Rouxel, J.; Coutard, J. G.; Gidon, S.; Lartigue, O.; Nicoletti, S.; Parvitte, B.; Vallon, R.; Zéninari, V.; Glière, A. *Sens. Actuators, B* **2016**, *236*, 1104−1110.
(20) Alahmari, S.; Kang, X.-W.; Hippler, M. *Anal. Bioanal. Chem.* **2019**, *411*, 3777−3787.
(21) Salter, R.; Chu, J.; Hippler, M. *Analyst* **2012**, *137*, 4669−4676.
(22) Keiner, R.; Frosch, T.; Massad, T.; Trumbore, S.; Popp, J. *Analyst* **2014**, *139*, 3879−3884.
(23) Hippler, M. *Anal. Chem.* **2015**, *87*, 7803−7809.
(24) Smith, T. W.; Hippler, M. *Anal. Chem.* **2017**, *89*, 2147−2154.
(25) Jochum, T.; Fastnacht, A.; Trumbore, S.; Popp, J.; Frosch, T. *Anal. Chem.* **2017**, *89*, 1117−1122.
(26) Gordon, I. E.; Rothman, L. S.; Hill, C.; Kochanov, R. V.; Tan, Y.; Bernath, P. F.; Birk, M.; Boudon, V.; Campargue, A.; Chance, K. V.; Drouin, B. J.; Flaud, J.-M.; Gamache, R. R.; Hodges, J. T.; Jacquemart, D.; Perevalov, V. I.; Perrin, A.; Shine, K. P.; Smith, M.-A. H.; Tennyson, J.; Toon, G. C.; Tran, H.; Tyuterev, V. G.; Barbe, A.; Császár, A. G.; Devi, V. M.; Furtenbacher, T.; Harrison, J. J.; Hartmann, J.-M.; Jolly, A.; Johnson, T. J.; Karman, T.; Kleiner, I.; Kyuberis, A. A.; Loos, J.; Lyulin, O. M.; Massie, S. T.; Mikhailenko, S. N.; Moazzen-Ahmadi, N.; Müller, H. S. P.; Naumenko, O. V.; Nikitin,

DOI: 10.1021/acs.analchem.9b03284
Anal. Chem. 2019, 91, 13096−13104

A. V.; Polyansky, O. L.; Rey, M.; Rotger, M.; Sharpe, S. W.; Sung, K.; Starikova, E.; Tashkun, S. A.; Vander Auwera, J.; Wagner, G.; Wilzewski, J.; Wcisło, P.; Yu, S.; Zak, E. J. *J. Quant. Spectrosc. Radiat. Transfer* **2017**, *203*, 3−69.
(27) www.webbook.nist.gov/chemistry; accessed 10/16/2018.
(28) Loomis, W. F.; Magasanik, B. *J. Bacteriol.* **1967**, *93*, 1397−1401.
(29) Inada, T.; Kimata, K.; Aiba, H. *Genes Cells* **1996**, *1*, 293−301.
(30) Mostovenko, E.; Deelder, A. M.; Palmblad, M. *BMC Microbiol.* **2011**, *11*, 126.
(31) Grosz, R.; Stephanopoulos, G. *Biotechnol. Bioeng.* **1983**, *25*, 2149−2163.
(32) Sezonov, G.; Joseleau-Petit, D.; D'Ari, R. *J. Bacteriol.* **2007**, *189*, 8746−8749.
(33) Miller, C. G. Protein degradation and proteolytic modification. In *Escherichia coli and Salmonella: Cellular and Molecular Biology*, 2nd ed.; Neidhardt, F. C., Curtiss, R., Ingraham, J. I., Lin, E. C. C., Low, K. B., Magasanik, B., Reznikoff, W., Riley, M., Schaechter, M., Umbarger, H. E., Eds.; ASM Press: Washington, D.C., 1996; pp 938−954.
(34) Li, Z.; Nimtz, M.; Rinas, U. *Microb. Cell Fact.* **2014**, *13*, 45.
(35) Wang, J.; Atolia, E.; Hua, B.; Savir, Y.; Escalante-Chong, R.; Springer, M. *PLoS Biol.* **2015**, *13*, e1002041.
(36) Fernández-Coll, L.; Cashel, M. *Front. Microbiol.* **2018**, *9*, 1802.
(37) Chu, D.; Barnes, D. J. *Sci. Rep.* **2016**, *6*, 25191.

DOI: 10.1021/acs.analchem.9b03284
Anal. Chem. 2019, 91, 13096−13104